18

Ceramic-Metal Joining Using Active Filler Alloy-An In-Depth Electron Microscopic Study

Abhijit Kar[1*] and Ajoy Kumar Ray[2]
[1]*J.B.Centre of Excellence, Jagadis Bose National Science Talent Search,*
[2]*Material Science & Technology Division,*
National Metallurgical Laboratory (CSIR),
India

1. Introduction

Joining of materials provides a means of fabricating structures, where difficulty is encountered to make one piece directly. Very often joining can be considered to be less expensive than making single piece structure for many intricate shaped components. Brazing is one of the most important techniques for joining various materials especially ceramics. To fabricate near net shape joined component or to make prototypes of intricate shapes, joining of ceramics to ceramics/metals, brazing has been considered as the most frequently used technique. Due to their excellent high temperature strength, resistance to corrosion and wear, application of ceramics in structural components, has received extensive attention in recent decades. However difficulties on joining ceramics with metals restrict their use in many occasions. The ability to produce a reliable ceramic-ceramic/metal and composite joint is a key enabling technology for many productions, prototype and advanced developmental items and assemblies. Thus it becomes an interesting challenge to the researchers for ceramic-metal joining.[1,2] Amongst several ceramic joining processes, *active metal brazing* is one of the most extensively used joining techniques for metal-ceramic joining. In this process, bonding is promoted by the use of an active filler alloy. The active filler alloy containing a small amount of an active element which is capable of reacting with the ceramic substrate facilitates joining.[3-12]. Characteristics of filler alloy play a significant role in obtaining unique joining properties. Filler alloy should have the liquidus temperature, below the melting point of the substrate to be joined and also must be capable of producing joint at a temperature where the properties of base materials are not degraded

Joining of two materials, whether homogeneous or heterogeneous almost always causes changes in the microstructure and mechanical properties in the vicinity of joint. A better understanding of the microstructure and mechanical property relationships of the braze joints will give valuable feed back to the materials developmental activities both in conventional and new material areas.[13] In case of metal-ceramic joining, interfaces exhibit

* Corresponding Author

abrupt discontinuity of properties, e.g. crystallographic, electronic, mechanical, thermodynamic and thermo-chemical.[3,14-16] Successful joining depends mainly on the interface characteristics; namely its mechanical behaviour, which in turn is highly dependent on the microstructural morphology and on how the discontinuity of the properties is accommodated by the interface. Therefore, the knowledge of the reaction product nature, their distribution and its chemical and mechanical characteristics are of fundamental interest.

2. Mechanism of ceramic brazing

Brazing of ceramic substrate to a metallic substrate is less studied. In case of joining ceramics, many attempts have been made to improve the wettability between ceramic to filler alloy by reducing contact angle (θ) between *solid-liquid*. Metalizing process improves the wettability of ceramic surfaces with conventional filler alloys. To ensure the production of reliable ceramic to metal seals, most of the cases ceramic surfaces are coated with Ni, Cu and other metals for metallization. The coating is usually done by electrolytic plating, gas-phase precipitation, thermal spraying, plasma spraying, ionic plating, electron and laser-beam techniques.[17,18] The widely used method for joining ceramic to metal is the multi-step moly-manganese process, where a moly-manganese coating is applied on the ceramic surface to induce wetting properties and the assembly is joined by brazing,[19-23].

One of the basic problems in brazing of ceramics without metallization lies in their poor wetting by the conventional brazing alloys. The wetting behaviour of the ceramic surfaces by the liquid metals has long been the subject of study. It is well known that in many systems the wetting process depends on the chemical reactions occurring at the solid-liquid interface. Normally, the active filler alloys used for direct joining contain reactive elements such as Ti, Zr, Ta etc. These elements react with the ceramic and thus provide a good joint. [24] The mechanism may be describe that at elevated temperatures, the active element reacts with the non-metallic component of the ceramic to form a complex interfacial layer that is wettable by other constituents of the brazing alloy.

Many researchers used laminated filler alloys [25-27] to join ceramics. In this process the active element layer (e.g. Ti foil) in general is kept at the sandwich condition between two layers of eutectic alloy (e.g. Ag-Cu). In general this is a suitable process where the gap between the two substrates are substantial, Since there are at least three layers, in all practical purposes it is to use very difficult to precisely maintain the dimension of the foils.

Considering all the above mentioned limitations now a day the most widely used method is active metal brazing technique. In this chapter readers should consider active filler metal and active filler alloy is synonymous

3. Selection of the filler alloy

Some of the Ag-based active filler metals are ductile and adaptable to braze materials such as Al_2O_3, Si_3N_4, SiC, partially stabilized zirconia (PSZ) as well as many other refractory ceramics.[28,29] One of the most commonly used active constituents is Ti, this can facilitate wetting of the majority of engineering ceramics. The reactivity and wetting behaviour of

filler alloys are considerably increased by small additions of active metal such as Ti or Zr. The driving force for the reactivity is the high oxidation potential of Ti, which results in a redox reaction with the ceramic. Merely increasing the concentration of titanium in the alloy prone to increase the liquidus temperature and the likelihood of alloy embrittlement by the formation of excessive amount of intermetallics / oxides of titanium. Therefore, the amount of Ti in the Ag-Cu base alloy should be optimized before application.

The choice of the reactive element depends on several other factors [30]. Fox and Slaughter had developed a few active metal alloys, like Ti-28Ag-4Be and Ti-49Cu-2Be for joining graphite to metal and these are mainly used for nuclear reactor technology.[31] Mizuhara et al.[32] and Xu et al.[33] had prepared Ag-Cu eutectic braze alloy containing up to 5% Ti. These alloys were prepared either as a tri-foil, consisting of a titanium sheet that is roll-clad with the silver-copper alloy, or as a silver-copper alloy wire with a titanium core. Similarly in certain processes, Ti vapour coating on the ceramic surface prior to brazing improved their wetting characteristics and permitted braze filler metals to adhere strongly to the ceramics. [34, 35]

Currently the active filler alloys have been identified as potential materials for ceramic brazing, however the details about the identification of the phases in the reaction layers and the extent to which microstructure in the reaction layers influences wetting, adhesion properties and bond strength, are still largely unresolved.[36]

3.1 Experimental procedure

In the current chapter we have considered TiCuSil *[97(72Ag28Cu) 3Ti]* as the active filler alloy in order to braze Al_2O_3 with 304SS. Active filler alloy was prepared in melting and casting route. Conventional chemical analysis shows that the concentration of Ag, Cu, and Ti in the brazing alloy is 71.8 wt%, 25.1 wt% and 3.1 wt% respectively. Substrates and the alloys were polished and cleaned ultrasonically using ethanol and acetone. The roughness of the cleaned substrates was measured by a profilometer (Taylor Hobson precision, Taylsurf Series 2) with a resolution of 16nm. The dimensions and surface roughness of the materials used for joining were as follows:

Al_2O_3 = 10(l) x 8(b) x 5(t) mm;
304 SS = 10(l) x 8(b) x 5(t) mm;
filler alloy = 9(l) x 7(b) x 0.4(t) mm;
roughness (Ra) of the Al_2O_3 was 0.46 μm and that of the SS was 0.16 μm.

The filler alloy was sandwiched between the alumina and the stainless steel substrates. The assembly was placed in a graphite resistance furnace (ASTRO, Thermal Inc., USA). A fixed load of ~8MPa was applied over the sample to keep the assembly aligned properly during brazing. This ensured a proper contact between the surface of the substrates and the filler alloy. This load also facilitates some interfacial reactions. The furnace was heated at the rate of 6^{O}C/min. till it reached the maximum brazing temperature of 1000^{O}C. Before the cooling starts it was kept at 1000^{O}C for 15 minutes. The cooling rate was maintained at 3^{O}C/min. upto 200^{O}C and thereafter it was furnace cooled. Before heating, the furnace was purged with argon gas (IOLAR I), and throughout the brazing cycle ~50-millitorr pressure was maintained through a rotary pump.

It is also important to note that, microstructures presented and described in this chapter are mostly from the samples brazed at 1000^{O}C. It was found that for the above considered specifications of the substrates and fillers, brazing carried out at 1000^{O}C produced the best result.

4. Interfacial reaction products

Joining of ceramics requires reaction between the substrate and the filler alloy to form an interface. The formation of reaction products provides the bond strength for the brazed sample. The reaction depends on the wetting behaviour of the ceramic and the filler alloy.

The nature of the reaction product depends on several factors. Most importantly concentration of the filler alloy used and the reactivity of the filler alloy with the substrates (ceramic /metal) apart from other different physical factors such as time, temperature profile, atmosphere ect. The reaction products that are formed mostly the active element bearing phases. Often the quantity of these phases is also affect the quality of the brazed joint. Thus it is the most vital factor in terms of qualitative and quantitative analysis of these phases, in order to determine the quality of the overall brazed interface.

Ti is most widely used as an active element of different filler alloys. The reactive Ti wets the ceramic/alumina and metal surfaces by reducing them, hence the reaction products are formed which facilitate the further bonding between the two substrates. [37] Wetting depends on the interfacial reactions and the thermodynamic activity of the Ti (a_{Ti}). The a_{Ti} depends on the mole fraction of the Ti (χ_{Ti}) in the melt. [38]

For alumina brazing, once Ti diffuse towards the alumina substrate, it reduces the alumina, hence forms the different reaction products. Sequentially the reactions that are believed to be taken place between the alumina and the active filler alloy are as follows,

$$4Al_2O_3 + 6Ti = 8Al + 6TiO + 6O \quad (1)$$

$$2Al + Ti + 5O = Al_2TiO_5 \quad (2)$$

$$3Ti + 3Cu + O = Cu_3Ti_3O \quad (3)$$

It is interesting to note that all the reaction products found at the alumina interface is obviously Ti bearing, thus the diffusion zone is considered with respect to the variation of the concentration gradient of the Ti across the interface which has been observed in EPMA concentration penetration profile (CPP) [39-46].

The formation and growth of the reaction layer are controlled mainly by diffusion of titanium through the continuous reaction layer. From the EPMA-CPP of Al_2O_3 to the 304SS, it is observed that the Ti diffusion mostly follow a Gaussian path [39]. By transmission electron microscopy (TEM) analysis two different phases like Cu_3Ti_3O (Figure 1. TEM) and Al_2TiO_5 (Figure 2. TEM has been confirmed apart from TiO (Figure 3. TEM) on the interface adjacent to alumina In fact the presence of these phases is more feasible as Ti has better chemical affinity towards Al, oxygen and Cu rather than Ag. It is interesting to note that so far no other report for the existence of Al_2TiO_5 phase within the interface adjacent to Al_2O_3.

Presence of these phases has been proved to be beneficial for the interface design Table 1. (Thickness and strength). Exhibits how reaction products and their thickness changes with temperature and its effect on mechanical property.

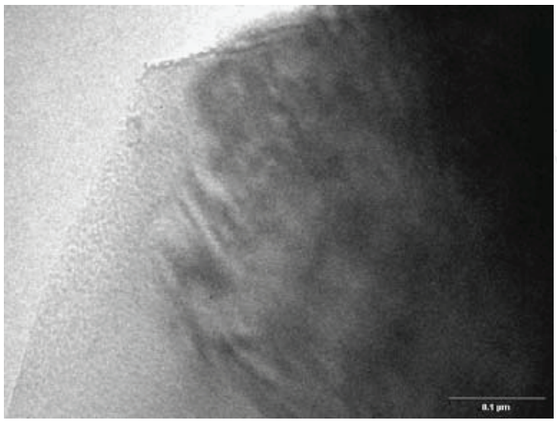

(a)

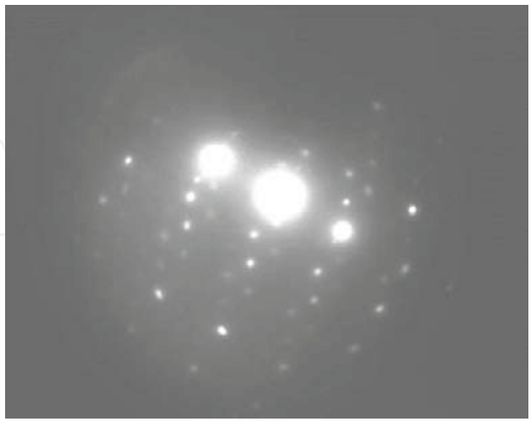

(b)

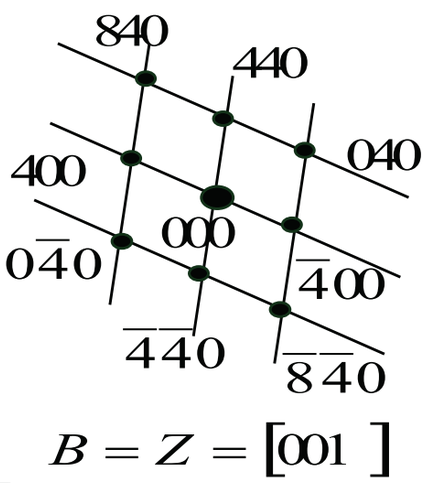

(c)

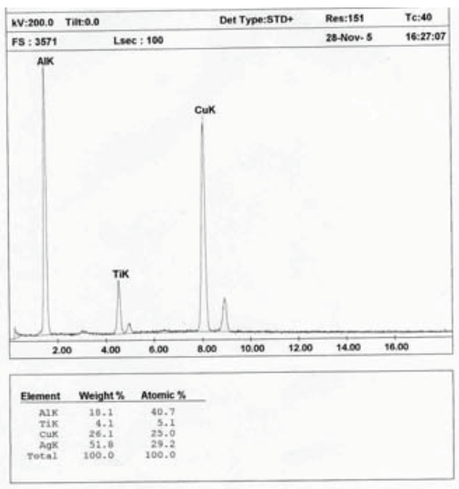

(d)

	Observed/ Experimental lattice spacing values (d)	Standard values at JCPDS file	*(hkl)*	α_1 experimental from the SADP	α_1 Theoritical	α_2 experimental from the SADP	α_2 Theoritical
R_1	$d_1 = 2.79$	2.814	400	34°	36°	29°	31°
R_2	$d_2 = 1.26$	1.258	840				
R_3	$d_3 = 2.0$	1.99	440				

Fig. 1. (a) TEM micrograph (b) SAD pattern (c) Schematic diagram of the diffraction array (d) corresponding quantitative EDS analysis and the alumina interface; confirms the presence of cubic **Cu_3Ti_3O** phase in the interface.

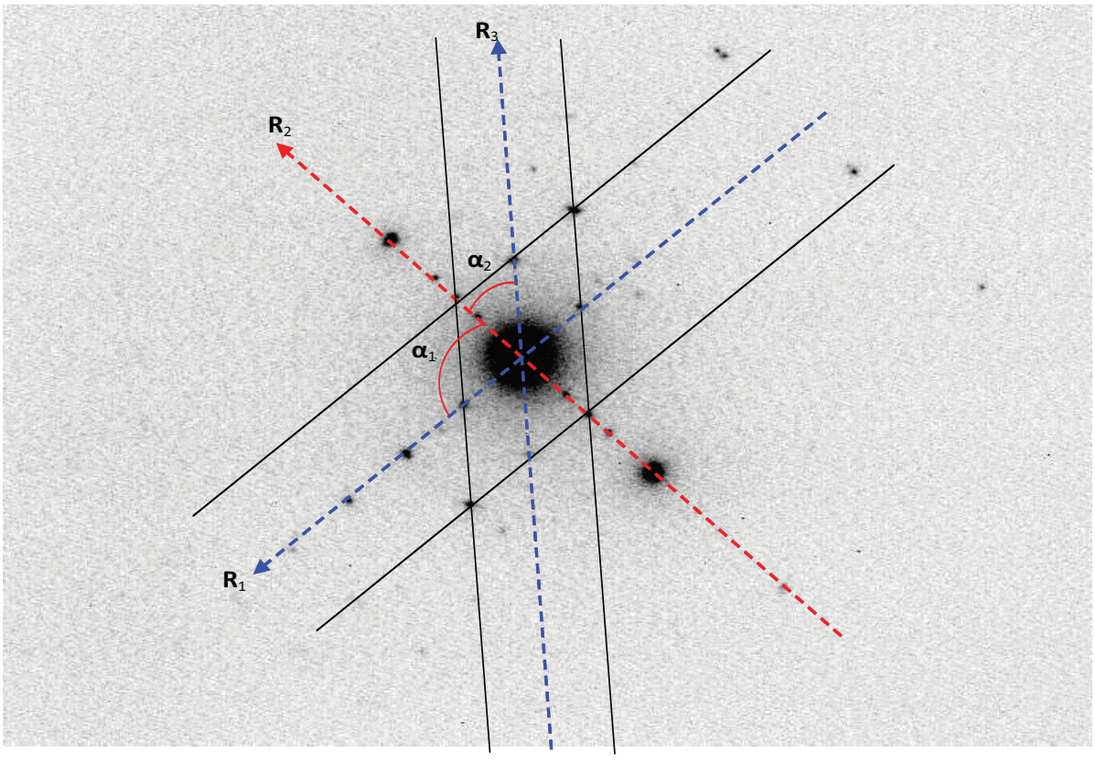

	Observed/ Experimental lattice spacing values (d)	Standard values at JCPDS file	*(hkl)*	α_1 experimental from the SADP	α_1 Theoritical	α_2 experimental from the SADP	α_2 Theoritical
R_1	$d_1 = 1.76$	1.784	-025	81°	79.8°	44.5°	46°
R_2	$d_2 = 1.544$	1.585	222				
R_3	$d_3 = 1.308$	1.305	-243				

Fig. 2. Selected Area Diffraction (SAD) pattern and Schematic diagram of the diffraction array; table below exhibits corresponding lattice parameters, theoretical and experimental values; confirms the presence of orthorhombic **Al_2TiO_5** phase in the interface. Here, the diffraction array has been marked ($\mathbf{R_1}$, $\mathbf{R_2}$, $\mathbf{R_3}$) and angles have been denoted by $\boldsymbol{\alpha_1}$, $\boldsymbol{\alpha_2}$

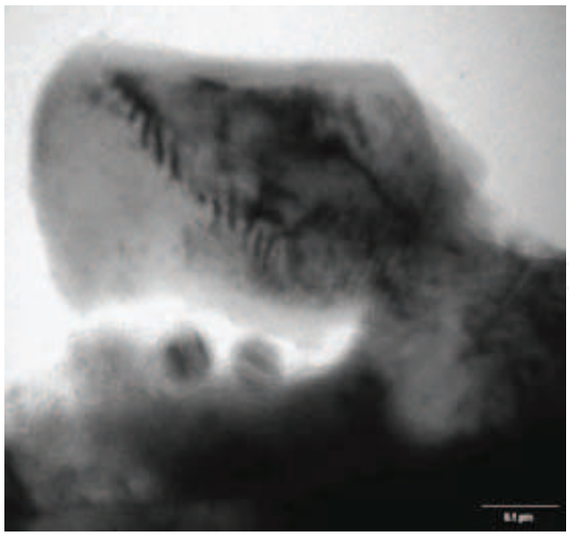

(a)

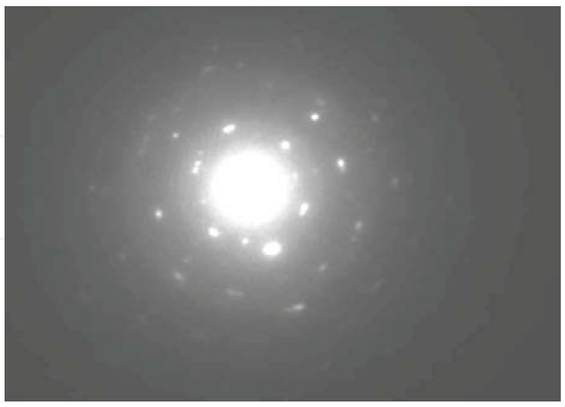

(b)

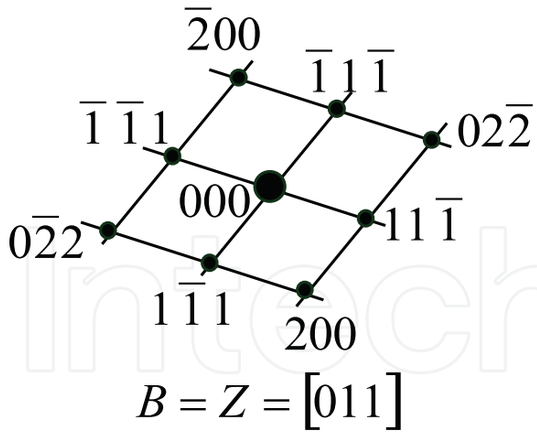

(c)

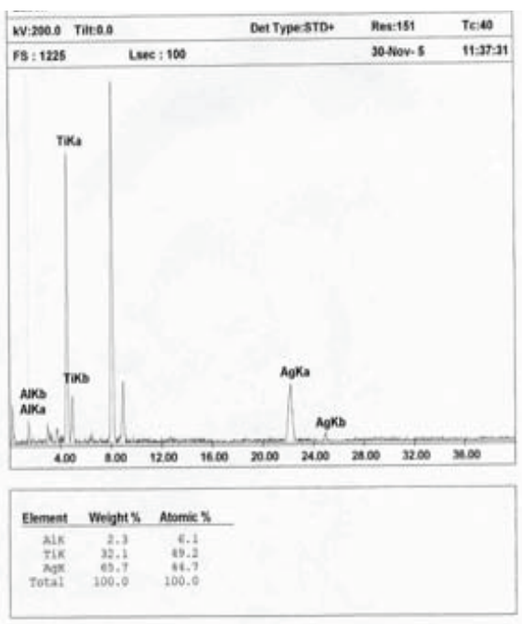

(d)

Fig. 3. (a) TEM micrograph (b) SAD pattern (c) Schematic diagram of the diffraction array (d) corresponding quantitative EDS analysis and the alumina interface; confirms the presence of cubic **TiO** phase in the interface.

Location	Phase/layer of reaction products	**Average Atomic Number**	Approximate Thickness **(μm)**			
			800 °C	**900 °C**	**1000 °C**	**1100 °C**
Ceramic Substrate	Al_2O_3	10	--	--	--	--
Alumina Interface	TiO (L_1)	15	0.8	3.0	2.3	Not Distinguishable
	Al_2TiO_5 (L_2)	11	--	Scattered Islands	6.3	
	Cu_3Ti_3O (L_3)	23	3.0	4.5	5.7	
	Total Thickness (μm)	--	3.8	7.5	14.7	4.2
Residual Filler alloy	Ag-Cu-Ti	--	484	350	280	85
SS Interface	$Fe_{35}Cr_{13}Ni_3Ti_7$ (L_4)	25.17	3.0	4.0	5.5	3.9
	FeTi (L_5)	24	4.8	7.5	9.5	7.7
	Total Thickness (μm)	--	7.8	13.7	15	11.6
Metal Substrate	Major constituent, Fe	26	--	--	--	--
Total Joint thickness	--	--	495	370	310	215
Shear strength of the joint (MPa)	--	--	**57**	**64**	**94**	**46**

Table 1. Thickness of different reaction product layers, residual filler, total joint, and shear strength of the brazed samples prepared at different temperatures.

Kar et al. [40] showed that in case of Al_2O_3-304SS brazed couple, it consists of two different interfaces. One is alumina interface and the other is SS interface. This complies with the fact that the reaction products formed in this interface i.e. TiO, Cu_3Ti_3O and Al_2TiO_5 [13,40] exhibits gradually decrease in hardness. The SS interface on the other hand found to be consists of two different reaction product layers, e.g. FeTi and $Fe_{35}Cr_{13}Ni_3Ti_7$ [47,40] all these phases have been identified and confirmed by X-ray diffraction analysis (Figure 4 (a, b). XRD) and transmission electron microscopy (Figure 5. TEM FeTi) and Figure 6. TEM $Fe_{35}Cr_{13}Ni_3Ti_7$).. In general, the oxides are more brittle than intermetallics; hence the hardness of the interface at the ceramic side is more than that of, at the metal side. As a result, ceramic interface becomes more susceptible to thermal or mechanical shock.

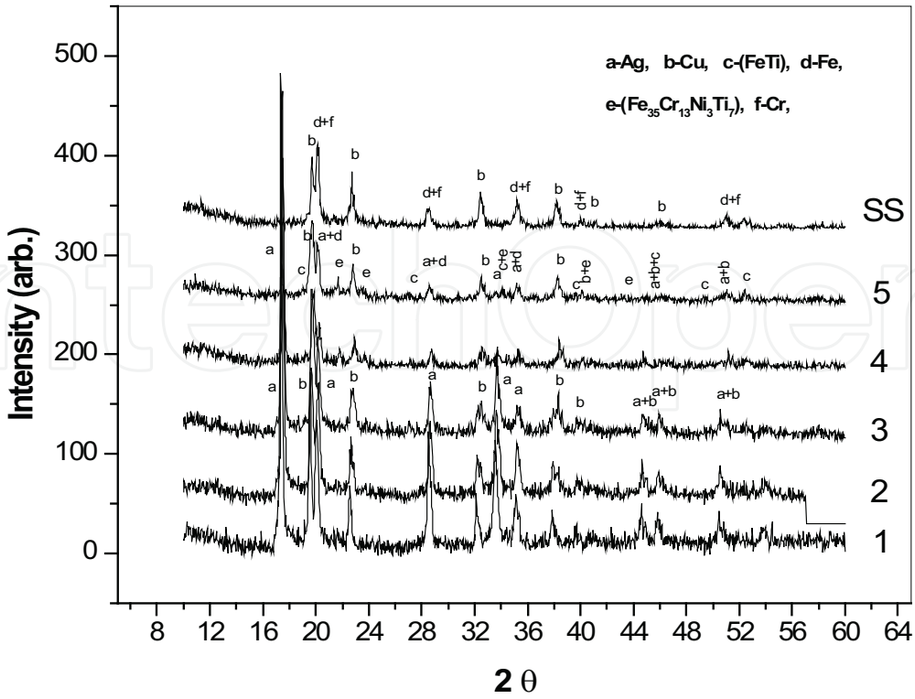

Fig. 4. (a) X-Ray diffraction patterns (XRD) of Al_2O_3 –304 SS brazed joint. Some of the most relevant diffraction patterns taken from the SS interface are depicted. MoK_α radiation

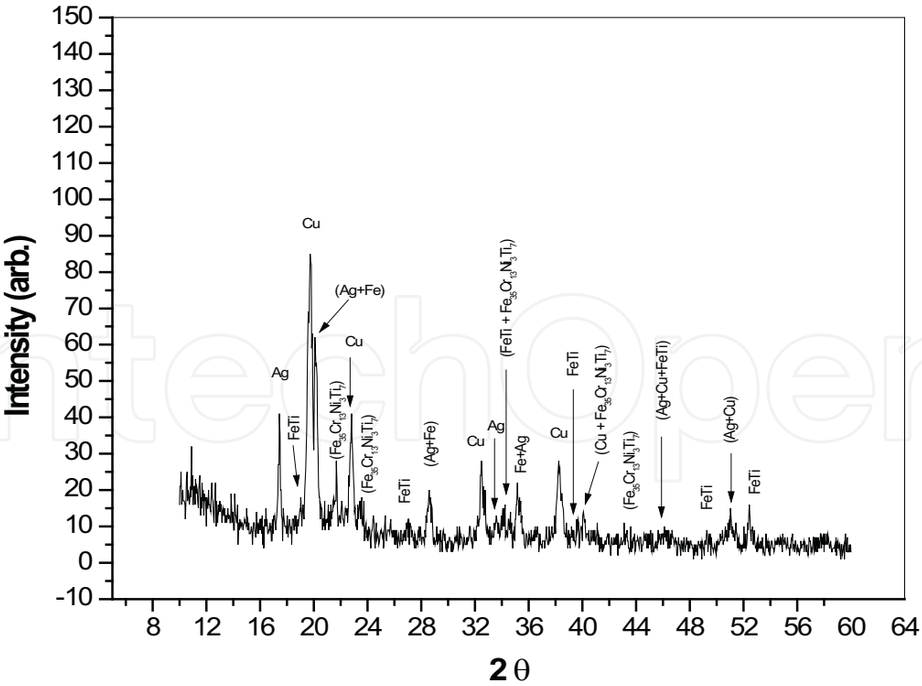

Fig. 4. (b) X-ray diffraction patterns (XRD) of Al_2O_3– SS brazed joint: pattern '5' of the above figure adjacent to SS interface. MoK_α radiation, Figure identifies the presence of FeTi and $Fe_{35}Cr_{13}Ni_3Ti_7$

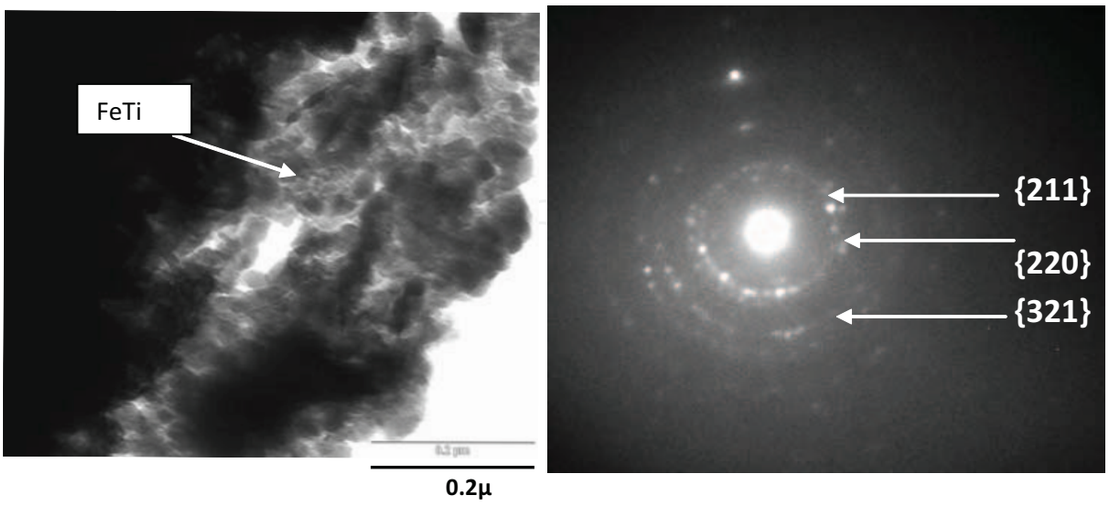

(a) (b)

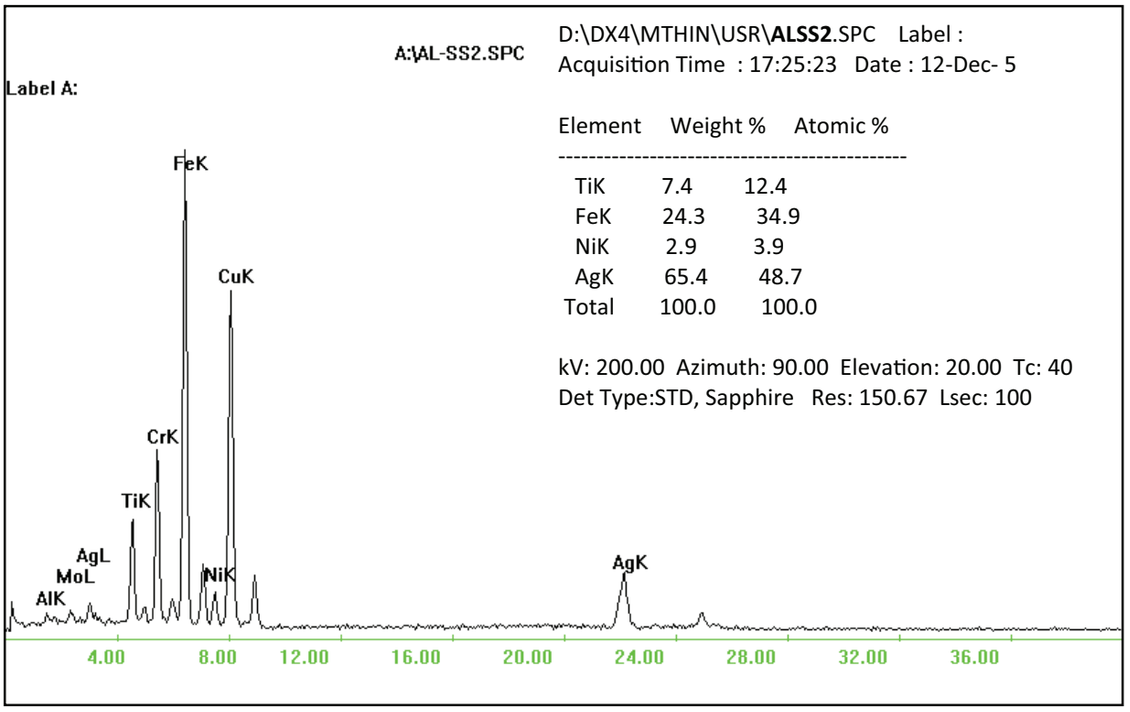

(c)

Fig. 5. TEM micrograph and SAD patterns obtained from the SS interface (a) TEM micrograph and (b) diffraction pattern of **FeTi** phase. (c) Exhibits the EDS analysis obtained from the area from which the diffraction pattern has been recorded. Spots marked by circle in the SAD patterns are from Ag with zone axis B=z=122

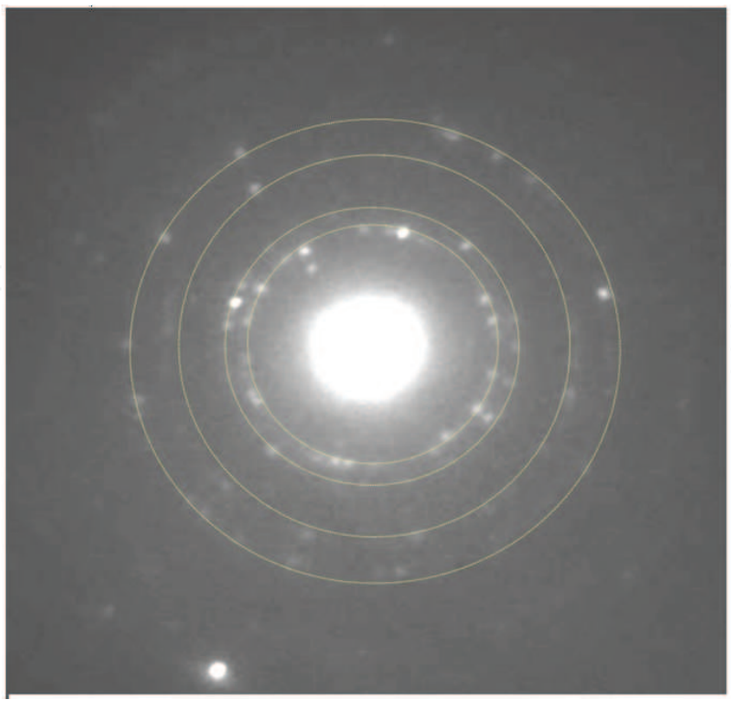

(a)

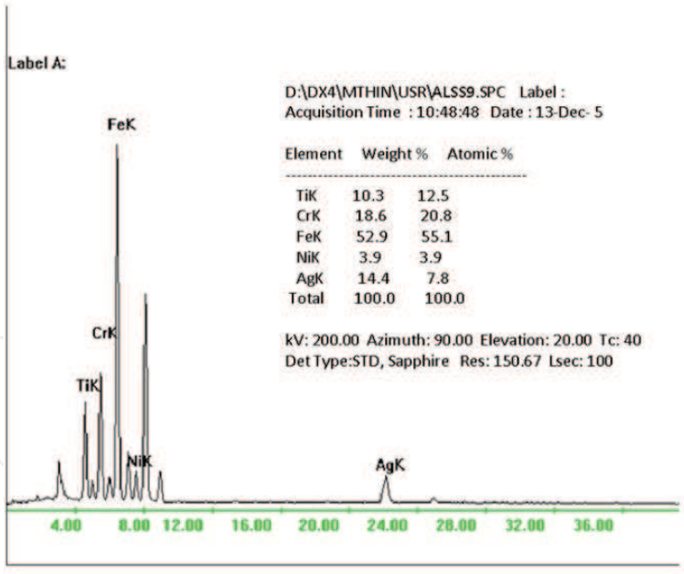

(b)

Fig. 6. TEM- EDS analysis of the cubic $\mathbf{Fe_{35}Cr_{13}Ni_3Ti_7}$ phase. Diffraction array has been marked by dotted circular line

As the thicknesses of the interfaces are quite narrow and often there is no sharp boundary, it is always an extremely difficult task to know particularly about the volume and relative positions. Recently Kar et al. [48] showed that the high resolution back scattered SEM images

(Figure 7. SEM Alu & Figure 8. SEM SS interface) of the interface can be used to determine the respective location of different phases present in the interfacial reaction products zone. From the principle of electron microscopy, it is known that the elements with higher atomic number experience more interaction with the bombarded electrons, thus the number of scattered electrons is also high; as a result bright images are formed. On the other hand elements with lower atomic number, will have lesser electron-mass interaction, as a result the amount of electron scattered will also be less, hence produces darker images. Therefore, this principle of analyzing the different contrasts in the images and correlating the corresponding EDS results, the relative position of the phases present in the interface can be identify. Based on this it is concluded that TiO is formed adjacent to Al_2O_3, Cu_3Ti_3O is adjacent to the filler alloy and Al_2TiO_5 is between TiO and Cu_3Ti_3O phases. Using same technique they suggested that the formation of Al_2TiO_5 was initiated around 900^{O}C and grown fully at 1000^{O}C.[48] (Table 1)

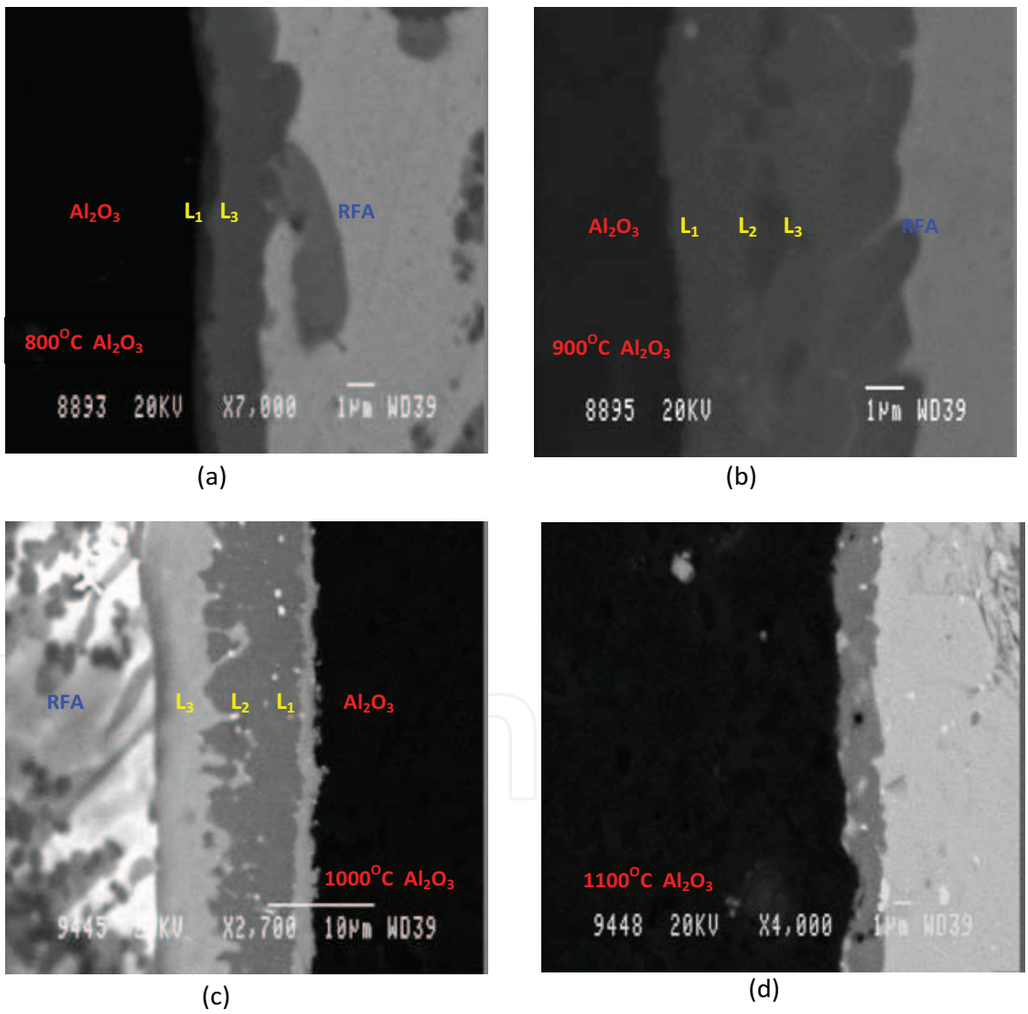

Fig. 7. SEM –BS images of the Al_2O_3 interface. Different reaction product layers can be clearly distinguished from the contrasts. Clock wise from the top left corner it is, sample brazed at (a) 800^{O}C, (b) 900^{O}C, (c) 1000^{O}C, (d) 1100^{O}C. *For abbreviation* L_1, L_2, L_3 please see table 1.

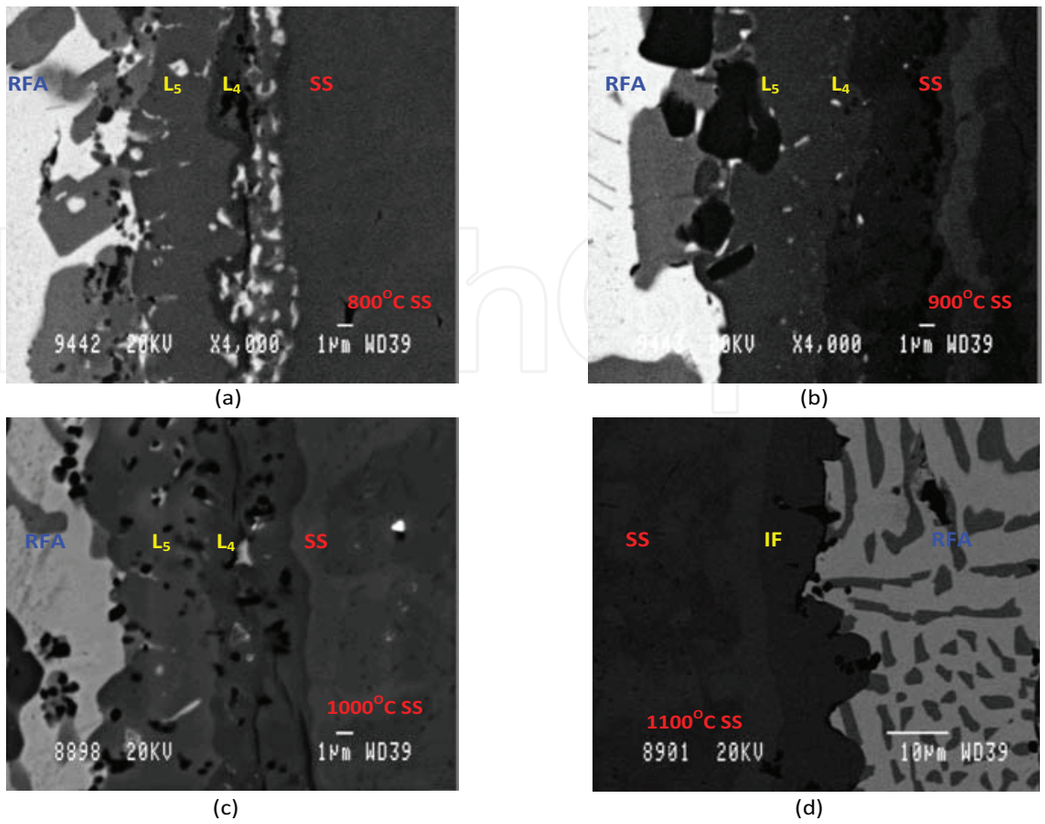

Fig. 8. SEM –BS images of the SS interface. Different reaction product layers can be clearly distinguished from the contrasts. Clock wise from the top left corner it is, sample brazed at 800°C; 900°C; 1000°C; 1100°C. *For abbreviation L_4, L_5 please see table 1.*

5. Phase identification

For any system, the presence of phases may be confirmed either by XRD, TEM or by Neutron diffraction studies; other methods can only help identify the existence of different phases within the system. To know the chemistry of the interface formed during brazing, it is very much necessary to determine the reaction products/phases present. As the thickness of the interfaces varies in the range of 7 to 15µm eventually the volume fraction of the reaction products are very small, hence the major peaks obtained by XRD are mostly either from ceramic, residual filler alloy or metal substrates. One of the easiest ways to get reasonably identifiable peaks either of the substrates was sliced orthogonally to the joint axis, approximately 0.2mm away from the interfacial reaction product zone. This enables to reach the interfacial reaction product layer by further mechanical grinding. This process gives better exposure to the interface, for the phase identification by XRD analysis. X-ray diffraction patterns can be recorded after removing each layer step in successive steps. The tentative thickness of each removed layer may be in the order of ≤1µm. The process is tedious and time consuming, but it could identify the reaction products present in the interface, The XRD patterns of the Al_2O_3 interface of the Al_2O_3-SS joint has been exhibited in the Figure 9. (a-c) represent mostly Al_2O_3 substrate, Figure 9(d,e) represents reaction products along with Al_2O_3, Ag, Cu. Whereas, Figure 19(f) represents residual filler alloy (mostly Ag-Cu after the diffusion of Ti). The interface adjacent to alumina was very thin and the concentration of reaction

products were also less in quantity, as a result, intensity of the XRD peaks observed are small. The small peaks that are observed in Figure 9(d) are identified as TiO, Al_2TiO_5 and Cu_3Ti_3O at the alumina interface. The crystal structure of Cu_3Ti_3O and Cu_2Ti_4O are quite similar and both have *Fd3m* space group. The lattice spacing (d) values of both the phases are also more or less identical although they differ in their relative intensities. Before confirming the presence of Cu_3Ti_3O instead of Cu_2Ti_4O, the "d" values and their relative intensities should be very carefully analyzed. In this regard EDS or EPMA results also provided some conclusive information as the Cu:Ti ratio are 1:1 and 1:2 for Cu_3Ti_3O and Cu_2Ti_4O respectively.[13]

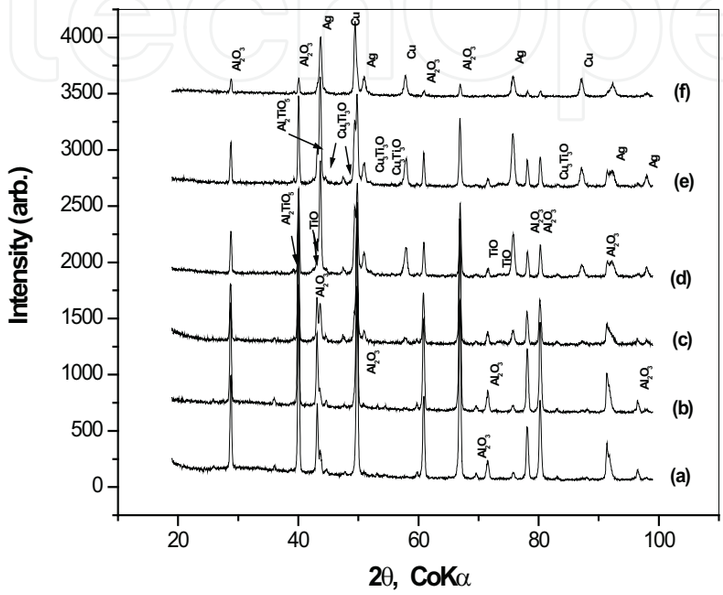

Fig. 9. XRD analyses around the Al_2O_3 interface of Al_2O_3-304 SS braze joint; (a-c) represent mostly Al_2O_3 substrate, (d & e) represent mostly interface along with Al_2O_3, Ag and Cu, (f) represents mostly the residual filler alloy.

It was suggested that Ti_3Cu_3O phase be developed through precipitation process. Karlsson et al.[49,50] suggested that Ti_3Cu_3O was isomorphous with cubic Fe_3W_3C and the phase is likely to be metallic in nature. The Ti_3Cu_3O structure was the same as that of many other transition-metal borides, carbides, nitrides and oxides, collectively known as η phases.[102] The Ti_3Cu_3O-phase layer may also provide a more gradual transition in physical properties and help to minimize the effect of local strains developed due to thermal expansion coefficient mismatches on adhesion.

The XRD peak intensities for the Al_2TiO_5 phase were also observed to be very low. This is because some of the peaks are merged with Al_2O_3 peaks. In the XRD patterns, many a times it is observed that some of the peak positions of two different phases superimposed to each other. This happens because of the similarities of the lattice parameters of those phases. In that case it is difficult to conclude the presence of a particular phase. In such cases, in order to conclude the reaction products present in the interface, it is recommended to verify its presence using different experimental, methods and instrumental techniques.

However, because of the higher volume fraction of the reaction products present in case of SS interface of Al_2O_3-SS joint; their identification is rather easier by XRD technique. Kar et al. suggested the presence of two phases namely $Fe_{35}Cr_{13}Ni_3Ti_7$ and FeTi in the SS interface using

Ag-Cu-Ti filler alloy, Figures 4(a,b). The phases are well distinguishable from the EDS and contrast in the BS-SEM images, Figure 8. The respective lattice spacing for different reaction products ('d' value) are tabulated in Tables 2 and 3 for Al_2O_3 and SS interfaces respectively.

Phase	Lattice spacing (d) Experimental	Lattice spacing (d) Standard in JCPDS	Diffraction plane (*hkl*)
TiO NaCl -type	3.30 2.41 2.10 2.08 1.48 1.47 1.35	3.32 2.41 2.098 2.069 1.485 1.467 1.365	*NaCl-type* structure
Al_2TiO_5 S.G.:Cmcm Orthorhombic	2.6 2.35 2.13 2.15	2.6 2.35 2.14 2.17	0 2 3 0 4 0 0 2 4 0 4 2
Cu_3Ti_3O S.G.:Fd3m *Cubic*	2.59 2.30 2.18 1.83 1.34 1.26	2.58 2.298 2.17 1.87 1.33 1.259	3 3 1 4 2 2 5 1 1 4 4 2 6 6 0 8 4 0

Table 2. Comparative lattice spacing values for different phases identified in the Al_2O_3 interface.

Phase	Lattice spacing (d) Experimental	Lattice spacing (d) Standard in JCPDS	Diffraction plane (*hkl*)
$Fe_{35}Cr_{13}Ni_3Ti_7$ Cubic SG: 143m	1.886 1.80 1.741 1.207 1.09	1.88 1.808 1.736 1.205 1.09	3 3 2 4 2 2 5 1 0 7 2 1 7 4 1
FeTi Cubic SG: Pm3m 19-0636	2.06 1.43 1.207 1.09 0.802	2.09 1.48 1.21 1.052 0.85	1 1 0 2 0 0 2 1 1 2 2 0 2 2 2

Table 3. Comparative lattice spacing values for different phases identified in the SS interface.

As it is mentioned that, although XRD analysis is the most commonly used technique to identify phases, for a smaller volume fraction of a phase, to render precise information about the reaction products formed in the interface, combined TEM studies (microstructure, diffraction and EDS) are necessary.

So far only one or two reports are available suggesting presence of such (Ti-Al-O) type of phase, but not specifically Al_2TiO_5. The presence of $Ti_3(Cu_{0.76}Al_{0.18}Sn_{0.06})_3O$ was reported by Santella et al.,[36] whereas, $(Ti, Al)_4Cu_2O$ was reported by Paulasto et al..[52] However, Ohuchi

et al. confirmed the formation of Ti_3Al phase while Ti was deposited on alumina at 1000^{O}C.[53] Ohuchi also reported that Ti reduces alumina and formed a stable Ti-Al compound with a fixed composition.

In case of the SS interface, presence of at least two distinct phases i.e., FeTi, and $Fe_{35}Cr_{13}Ni_3Ti_7$ has been confirmed by TEM analyses.[48] (Figure 5 and Figure 6).Three distinct rings from {211}, {220} and {321} are depicted in Figure 25 as observed in the SADP. Analysis of this SAD pattern confirms the presence of polycrystalline FeTi phase in the SS interface, local chemical composition this phase was also checked by EDS analysis. The zone axis of this cubic FeTi phase was found to be $[\bar{1}11]$. The crystal structure and also the lattice parameter of FeTi and NiTi are similar. However, higher concentration of Fe (~67 wt.%) than Ni (~10 wt.%) in the 304 SS substrate increase the possibility of FeTi formation rather than the metastable NiTi. TEM–EDS analysis as well as the Kikuchi pattern obtain from SEM-EBSD also confirm the presence of FeTi phase Figure 10.[54]

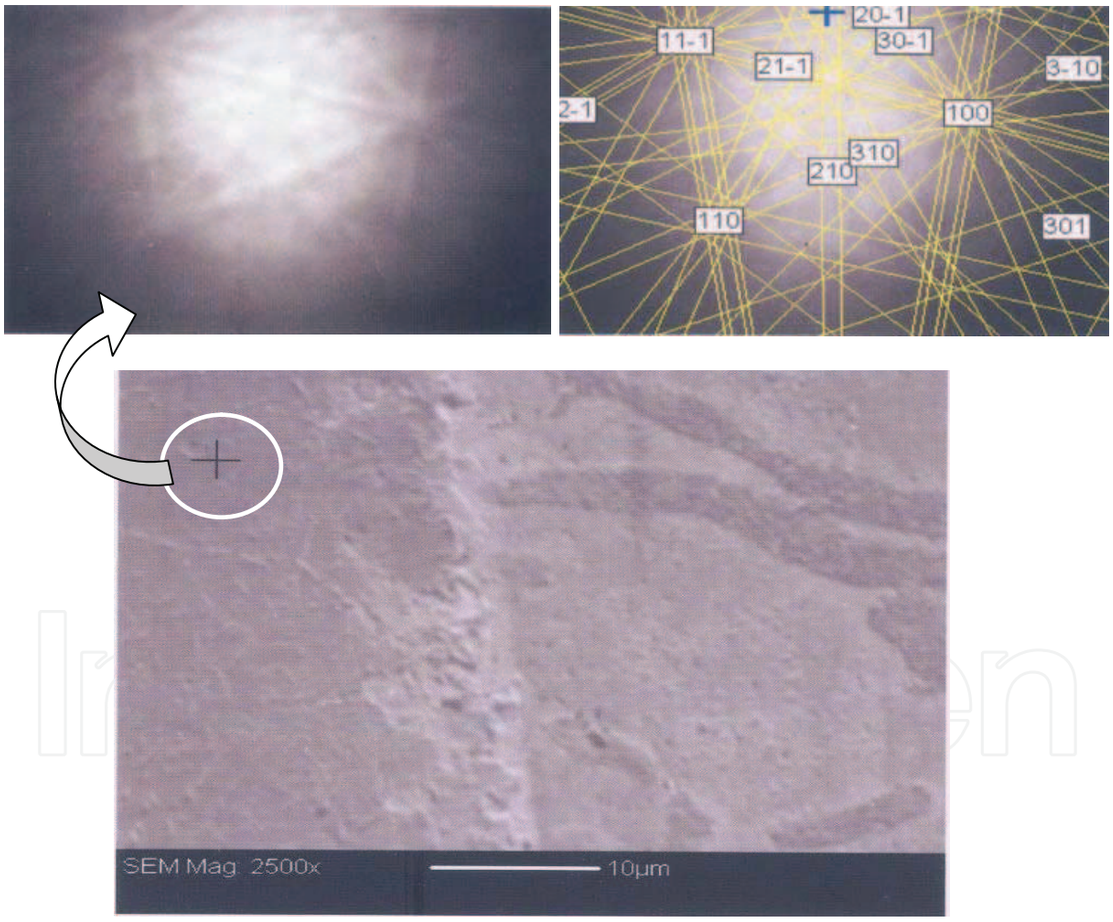

Fig. 10. SEM-EBSD Kikuchi patter confirms the presence of **FeTi** in the SS interface. Micrograph showing the position from which Kikuchi pattern has been recorded.

The presence of cubic $Fe_{35}Cr_{13}Ni_3Ti_7$ phase was also confirmed by the TEM analyses Figure 6.[48] Ti from the Ag-Cu-Ti filler alloy has been diffused towards SS side and reacted with the constituents present in the SS to form phases like FeTi and $Fe_{35}Cr_{13}Ni_3Ti_7$. Formation of these

phases causes bonding between SS and the residual filler alloy. Since these phases are considered to be intermetallics, they are harder than that of the substrate. The phases present in SS interface was polycrystalline in nature, whereas the SAD patterns recorded from the Al_2O_3 interface were observed to be single crystal spot pattern. Such variations in the particle sizes in the interface may be explained by their formation mechanisms. It has already been mentioned that at the juncture of Al_2O_3 and filler alloy, there should be unequal heat dissipation during cooling due to of the large difference of their CTEs. Such inhomogeneous cooling allowed the TiO, Al_2TiO_5 or Cu_3Ti_3O phases to grow into a bigger crystallite, after nucleation. Whereas the SS interface experience comparatively fast and uniform cooling, as in case of metal they have comparable CTEs. Such cooling does not provide time to the $Fe_{35}Cr_{13}Ni_3Ti_7$ or FeTi particles to grow and form bigger crystals. However, in most of cases secondary spots are observed in the diffraction SAD patterns and identified as either Ag or Cu.

6. Microstructure of the interface

Many investigators have suggested that the reaction products and the microstructure affect the quality of a braze joint. In the literature, there are different suggestions and opinions about the reaction layers within the interface of Al_2O_3 - (Ag-Cu-Ti)- SS braze joints. Santella et al.[36] observed that adjacent to Al_2O_3, there was Ti-rich layer having face-centered-cubic (fcc) crystal structure with a lattice parameter of 0.423 nm and the phase was identified as oxygen-deficient γ-TiO. The width of that layer was 0.1 to 0.2μm. The next layer was ~3μm thick and separated the TiO layer from the metallic phases of the filler metal. The structure of this layer was identified as diamond cubic unit cell of space group Fd3m with a lattice parameter 1.137nm and the composition of the phase was Ti_3Cu_3O. Similarly, Janickovic et al.[55,56] confirmed that the layer adjacent to Al_2O_3 is fcc TiO with lattice parameter of 0.423 nm. Moreover, they had suggested that the next layer is a mixture of hexagonal Ti_2O_3 and Cu_2O. Based on thermodynamic study,[57] the high temperature γ-TiO can be stabilized with Ti_3Cu_3O at local thermodynamic equilibrium in the Ti-Cu-O ternary system, when the chemical activity of titanium is low. Santella et al.[36] and Yang et al.[58] reported that aluminum concentration in the layer containing Ti_3Cu_3O phase, was relatively high and confirmed that the reduction of alumina surface layer occurred during the brazing process because the braze alloy originally contained no aluminum. As a result of this redox reaction, γ-TiO formed directly on the alumina surface and the reduced aluminum formed a solid solution with Ti_3Cu_3O in the next reaction layer. It was found that the Ti activity and the activity coefficient in the eutectic Ag-Cu melts increases with the increase of Ti concentration and showed a negative deviation from ideal solution at 1000^{O}C. However, Pak. et al.[59] found that the equilibrium oxide phase formed by the reaction of Ti in the Ag-Cu alloy melts with an Al_2O_3 crucible was Ti_2O, and the activity coefficient of Ti showed a positive deviation from ideal solution behaviour at 1000^{O}C. The activity coefficient of Ti at infinite dilution is about 0.076 relative to pure solid Ti and it decreases with the increment of Cu concentration and increases with the increment of Ag concentration.[60]

The interfacial reaction between Al_2O_3 and Ag-Cu-Ti alloy was investigated by Hongqi et al..[61] They reported that the joining conditions have a larger influence on the interfacial reaction. As the temperature and holding time are increased, the reaction layer thickness was increased but the rate of increment decreased when the temperature and time increased further. This may be due to the decrease in viscosity of the filler alloy in liquid state. With the increase of processing temperature, this less viscous filler alloy squeezed out from the

intermediate place between the two substrates and results thinner interface.[54] The layer thickness was mainly controlled by the diffusion of titanium through the reaction layers. The reaction products were Cu_2Ti_4O and AlTi at or below 950^{O}C K. However, in the interface there were two distinct layers at or above 900^{O}C. One layer in the vicinity of the Al_2O_3 consisting mainly of Ti_2O and TiO.

According to Hongqi et al. analyses of interfacial microstructures and morphologies, a lower or a higher brazing temperature and shorter or a longer holding time were disadvantageous for stable and reliable joined interface. However, there was no evidential or supporting experimental information made by Hongqi et al.. In general it may be mentioned that the lower processing temperature does not provide sufficient driving energy to produce a strong bonding interface. As it is mentioned earlier that at higher temperature, the molten filler alloy could not sustain to produce sufficient reaction products for a reliable joint. There should be an optimum brazing temperature and holding time for sound joint.

Kritsalis et al. found that there were two distinct layers between the Al_2O_3 and the alloy in the Cu-Ti/Al_2O_3 system.[62] One layer near the Al_2O_3 was titanium monoxide, $TiO_{1\pm x}$, with $x \leq 0.05$ and another layer near the filler alloy corresponds to the compound Cu_2Ti_2O. Cho et al. found that δ-TiO and γ-TiO phases were present at the interface of Al_2O_3 / Ag-Cu-0.5Ti joints.[63]

Loehman et al. analyzed the cross section of an interface results due to the reaction between Ag-33.5Cu-1.5Ti alloy with a high purity Al_2O_3 for 30 min at 900^{0}C.[64] They found that, a complex sequence of reactions and elemental diffusion occurred between the braze alloy and the Al_2O_3. Adjacent to the Al_2O_3 an uneven 1-2μm thick layer of titanium oxide was found which contains some Al. The slight relative shift in the Ti and O profiles suggests a variable stoichiometry of titanium oxide with a decreasing O / Ti ratio away from alumina. The successive region, moving away from alumina, is a thick layer of ~5μm. It is primarily Cu-Ti intermetallics, followed by another 5μm thick layer that is mixed Cu-Ti alloy and Cu-Ag alloy. At the extreme end, Cu-Ag eutectic structure was observed. They had also reported that all of the Ti in the braze alloy was segregated to the alloy/Al_2O_3 interface. A thin layer of that Ti reacted with Al_2O_3 and the remainder formed a Cu-Ti alloy. With longer reaction times (30 min.), TiO_x reaction zone would be greater and that of Cu-Ti would be smaller. Although Loehman et al. did not suggest any results correspond to the joint strength. So it is difficult to conclude or suggest on the effect of longer holding time or formation of thicker TiO layer.

7. Conclusion

The interfaces, of any braze joint are the key areas to control the quality of a joint. It consists of different reaction products; hence, in order to get a good braze joint it is essential to characterize the interface and optimize the amount of reaction product formed in the interface. It is observed that presence of different reaction products at the interface of similar system has been reported by different researchers. This indicates, either the formation of the interface is highly sensitive to the processing parameters or difficult task to characterize the interface properly. Non-availability of the systematic analysis of metal-ceramic brazed interface data is also a constrain.

Here we have shown the results of a very systematically analyzed interface of alumina-304SS brazed sample. Electron microscopy and simultaneous X-ray diffraction analysis is found to be the most authentic tool to be used for characterization of such interface, where within a few micron interface, consists of multiple layered reaction products.

Hence we conclude that in depth microstrutural characterization using transmission electron microscopy and simultaneous XRD and electron microscopy can provide good and reliable result which help designing interface for even better mechanical and functional property for any metal ceramic brazing system

8. References

[1] A. Murari, H. Albrecht, A. Barzon, S. Curiotto, L. Lotto, *Vacuum,* 2003, *68*, 321.
[2] Jian Chen. Pan Wei, Qiang Mei, Yong Huang, *J. Euro. Ceram. Soc.*, 2000, *20*, 2685.
[3] A. Guedes, A. M. P. Pinto, M. Vieira, F. Viana, *Mater. Sci. and Engg. A*, 2001, 301 118.
[4] M. R. Rijnders and S. D. Peteves, *Scripta Mater.*, 1999, *41* 1137.
[5] M. A. Groeber, B. K. Haley, M. D. Uchic, D. M. Dimiduk, S. Ghosh, *Mater. Charact.*, 2006, *57,* 259.
[6] Caroline S. Lee, Sung-Hoon Ahn, Lutgard C. DeJoghe, Gareth Thomas, *Mater. Sci. and Engg. A*, 2006, *434,* 160.
[7] Michikazu Kinsho, Yoshio Saito, Zenzaburo Kabeya, Keisuke Tajiri, Tomaru Nakamura, Kazuhiko Abe, Taketoshi Nagayama, Daiji Nishizawa, Norio Ogiwara, *Vacuum,* 2004, *73,*187.
[8] Braze Alloys- Silver Solders; 'Brazing Tungsten Carbide and Ceramics for Saws, Tools, and Wear Analysis-Carbide Processors, Inc., Chapter-12 (Northwest Research Institute, Inc. / Carbide Processors, Inc. 3847 S. Union Ave. Tacoma, WA. 98409 800 346-8274).
[9] A. H. Elsaway, M. F. Fahmy, *J. Mater. Process. Techno*., 1998, *77,* 266.
[10] Chia-Hasiang Chiu, Chien-Cheng Lin, *J. Am. Ceram. Soc.*, (2006), *89,* 1409.
[11] Kun-Lin Lin, Chien-Cheng Lin, *J. Am. Ceram. Soc.*, (2006), *89,* 1400.
[12] A. Meier, P. R. Chidambaram, G. R. Edwards, *Acta Mater.,* 1998. *46*, 4453.
[13] S. Mandal, "*Studies on the physical and metallurgical properties of silver copper base system for brazing applications*"; Ph.D. thesis, Jadavpur University, Kolkata, India, 2004.
[14] K. Scott Weil, Christopher A. Coyle, Jens T. Darsell, Gordon G. Xia, John S. Hardy, *J. Power Sources,* 2005, *152,* 97.
[15] W. Cao, J. Zhu, Y. Yang, F. Zhang, S. Chen, W.A. Oates, Y.A. Chang, *Acta Mater.,* 2005, *53,* 4189.
[16] S. Schmidt, S. Beyer, H. Knabe, H. Immich, R. Meistring, A. Gessler, *Acta Austronautica,* 2004, *55*, 409.
[17] M. M. Schwartz, in *Brazing for the engineering technologist*, Publ. Chapman & Hall, London, UK, 1995.
[18] M. M. Schwartz, in *Ceramic Joining,* ASM International, Materials Park, Ohio, USA, 1990.
[19] A.G. Pincus, *Ceram. Age,* 1954, *63,* 16.
[20] K. Suganama, T. Okamoto and M. Shimada, *Commun. Am. Ceram. Soc.,* July 1983, C-117-118.
[21] J. F. Burgess and C. A. Neugebauer, "*Direct bonding of metal to ceramics for electronic applications*"; Advances in. Joining Technology, Burke et al. Eds., 1974.
[22] H. J. Nolte, *Metallized ceramic, U.S. Patent 2,667,432*, Jan26, 1954.
[23] K. Ettre, *Ceram. Age,* 1965, *81,* 57.
[24] M. Vila, C. Prieto, P. Miranzo, M. I. Osendi, A. E. Terry, G. B. M. Vaughan, *Nucl. Instruments and Methods in Phys. Research B*, 2005, *238*, 119.
[25] Yutai Katoh, M. Kotani, A. Kohyama, M. Montorsi, M. Salvo, M. Ferraris, *J. Nucl. Mater.,* 2000, *283-287,* 1262.
[26] J. W. Park, P.F. Mendz, T.W. Eager, *Acta Mater.,* 2002, *50*, 883.
[27] A.M. Glaeser, *Composite Part B,* 1997, *28B*, 71.

[28] R. Morrell, in *Joining to other components, Part I, an introduction for engineer and designer*, *Handbook of properties of technical and engineering ceramics*, London, 1985.
[29] C. R. Weymueller, *Weldg. Des. & Fab.*, 1987, 45.
[30] A. Xian and Z. Si, *J. Mater. Sci. Lett.,* 1991, *10*, 1315.
[31] C. W. Fox and G. M. Slaughter, *Weld. J.,* 1964, *43,* 591.
[32] H. Mizuhara and K. Mally, *Wed. J.,* 1985, *64*, 27.
[33] S. Xu and J. E. Indacochea, *J. Mater. Sci.*, 1994, *29,* 6287.
[34] E. F. Brush, Jr. and C. M. Adams, Jr., *Weld. J.,* 1968, *47*, 106.
[35] M. L. Santella, *Adv. Ceram. Matls.,* 1988, *3*, 457.
[36] M. L. Santella, J. A. Horton and J. J. Pak, *J. Am. Ceram. Soc.,* 1990, *73*, 1785.
[37] Coralie Valette, Marie-Francoise Devismes, Rayisa Voytovych, Nicholas Eustathopoulos, *Scripta Mater.,* 2005, *52*, 1-6.
[38] M. G. Nicholas, *Br. Ceram. Trans. J.*, 1986, *85,* 144.
[39] Abhijit Kar, S. Mandal, K. Venkateswarlu and Ajoy Kumar Ray*, Mater. Charact.,* 2007, *58*, 555.
[40] Abhijit Kar, Sanjay Chaudhuri, Pratik. K. Sen, Ajoy Kumar Ray, *Scripta Mater.,* 2007, *57*, 881.
[41] J. Zhang, Y.L. Guo, M. Naka and Y. Zhou, *Ceram. Intern.*, 2008, *34*, 1159.
[42] Abhijit. Kar, S. Mandal, R.N. Ghosh, T. K. Ghosh and A. K. Ray; *J. Mater. Sci.,* 2007, *42(14)*, 5556.
[43] Ulrich E. Klotz, Chunlei Liu, Peter J. Uggowitzer, Jörg F. Löffler, *Intermetallics,* 2007, *15*, 1666.
[44] P. He, J. C. Feng, H. Zhou, Mater. Charact., 2005, 54, 338.
[45] Yutaka Hiraoka, Susumu Nishikawa, *Internat. J. Refrac. Metals and Hard Mater., 14*, 1996, 311.
[46] Feng Gao, Hui Zhao, Dusan P. Sekulic, Yiyu Qian, Larry Walker, *Mater. Sci. and Engg A,* 2002,*337*,228
[47] Abhijit Kar and Ajoy Kumar Ray, *Mater. Lett.,* 2007, *61*, 2982.
[48] Abhijit Kar, Mainak Ghosh, Ashok Kumar Ray and Ajoy Kumar Ray, *Mater. Sci. Engg. A,*2008,*498*,283.
[49] N. Karlsson, *Nature,* 1951, *168,* 558.
[50] N. Karlsson, *J. Inst. Met.,* 1951, *79*, 391.
[51] J. W. Edington, in *Practical Electron Microscopy in Materials Science,* Vol. 2 (N.V. Philips) Eindhoven, 1975.
[52] M. Paulasto, J. Kivilahti, *J. Mater. Res.*, 1998, *13*, 343.
[53] F. S. Ohuchi and M. Kohyama, *J. Am. Ceram. Soc.,* 1991, *74,* 1163.
[54] Abhijit Kar, "*Studies on interfacial characterization of ceramic-ceramic/metal brazed joints*"; Ph.D. thesis,Jadavpur University, Kolkata, India, 2004
[55] D. Janickovic. P. Sebo, P. Duhaj and P. Svec, *Mater. Sci. and Engg. A,* 2001, *304-306*,569.
[56] P. Duhaj, P. Sebo, P. Svec and D. Janickovic, *Mater. Sci. and Engg. A,* 1999, *271*, 181.
[57] G. P. Kelkar, K. E. Spear and A. H. Carim, *J. Mater. Res.*, 1994, *9*, 2244.
[58] P. Yang, B. N. Turman, S. J. Glass, J. A. Halbleib, T. E. Voth, F. P Gerstle, B. Mckenzie, J. R. Clifford, *Mater. Chem. and Phys.,* 2000, *64*, 137.
[59] J.J. Pak, M.L. Santella and R.J. Fruehan, *Metall. Trans. B,* 1990, *12*, 349.
[60] L. Rongti, P. Wei, C. Jian and L. Jie, *Mater. Sci. and Engg. A,* 2002, *335,* 21.
[61] H. Hongqi, W. Yonglan, J. Zhihao and W. Xiaotian, *J. Mater. Sci.,* 1995, *30,* 1233.
[62] P. Kritsalis, L. Coudurier and N. Eustathopoulos, *J. Mater. Sci.*, 1991, *26*, 3400
[63] H.C. Cho and J. Yu, *Scripta Mater.,* 1992, 26, 797.
[64] R. E. Loehman and A. P. Tomsia, *Am. Ceram. Soc. Bull.,* 1988, *67*, 375.

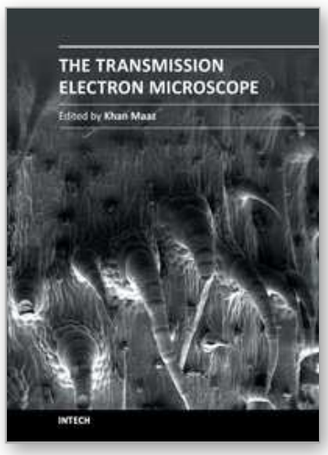

The Transmission Electron Microscope
Edited by Dr. Khan Maaz

ISBN 978-953-51-0450-6
Hard cover, 392 pages
Publisher InTech
Published online 04, April, 2012
Published in print edition April, 2012

The book "The Transmission Electron Microscope" contains a collection of research articles submitted by engineers and scientists to present an overview of different aspects of TEM from the basic mechanisms and diagnosis to the latest advancements in the field. The book presents descriptions of electron microscopy, models for improved sample sizing and handling, new methods of image projection, and experimental methodologies for nanomaterials studies. The selection of chapters focuses on transmission electron microscopy used in material characterization, with special emphasis on both the theoretical and experimental aspect of modern electron microscopy techniques. I believe that a broad range of readers, such as students, scientists and engineers will benefit from this book.

InTech Europe
University Campus STeP Ri
Slavka Krautzeka 83/A
51000 Rijeka, Croatia
Phone: +385 (51) 770 447
Fax: +385 (51) 686 166
www.intechopen.com

InTech China
Unit 405, Office Block, Hotel Equatorial Shanghai
No.65, Yan An Road (West), Shanghai, 200040, China
中国上海市延安西路65号上海国际贵都大饭店办公楼405单元
Phone: +86-21-62489820
Fax: +86-21-62489821

IntechOpen